PB82-155243

Interpretation of Complex Molecular Motions in Solution. A Variable Frequency Carbon-13 Relaxation Study of Chain Segmental Motions in Poly(n-alkyl methacrylates)

Florida State Univ., Tallahassee

Prepared for

Health Effects Research Lab.
Research Triangle Park, NC

11 May 77

U.S. Department of Commerce
National Technical Information Service
NTIS.

TECHNICAL REPORT DATA (Please read Instructions on the reverse before completing)		XX-81-070
1. REPORT NO. EPA-600/J-78-194	2. JOURNAL ARTICLE	3. RECIPIENT'S ACCESSION NO. PB82-155243
4. TITLE AND SUBTITLE Interpretation of Complex Molecular Motions in Solution. A Variable Frequency Carbon-13 Relaxation Study of Chain Segmental Motions in Poly(n-alkyl methacrylates)		5. REPORT DATE January 1982 6. PERFORMING ORGANIZATION CODE 025117
7. AUTHOR(S) George C. Levy, David E. Axelson, Robert Schwartz, and Jiri Hochmann		8. PERFORMING ORGANIZATION REPORT NO.
9. PERFORMING ORGANIZATION NAME AND ADDRESS Department of Chemistry The Florida State University Tallahassee, Florida 32306		10. PROGRAM ELEMENT NO. CCAE1A 11. CONTRACT/GRANT NO. Grant No: R804916
12. SPONSORING AGENCY NAME AND ADDRESS Office of Research and Development (RTP,NC) Health Effects Research Laboratory US Environmental Protection Agency Research Triangle Park, NC 27711		13. TYPE OF REPORT AND PERIOD COVERED 14. SPONSORING AGENCY CODE EPA-600/11
15. SUPPLEMENTARY NOTES Published In: Journal of the American Chemical Society 100(1): 410-424, 1978		

16. ABSTRACT

An extensive variable temperature study of poly(n-butyl methacrylate) and poly(n-hexyl methacrylate) at two widely separated frequencies (67.9 and 22.6 MHz) has revealed that a model requiring a nonexponential autocorrelation function, or, its mathematical equivalent, a distribution of correlation times, describes the NMR parameters obtained for the backbone carbons. However, frequency-dependent spin-lattice relaxation time (T_1) and nuclear Overhauser effect (NOE) behavior observed for all side-chain carbons, including the terminal methyls, with NT_1s of the order of 20s, could not be described in terms of present theoretical approaches. A new model developed retains the distribution of correlation times for the backbone carbons and incorporates the effects of multiple internal rotations about the carbon-carbon single bonds for the side-chain carbons. This model predicts a substantial frequency dependence for broad distribution widths which can quantitatively reproduce almost all of the observed data. For the highest temperatures attained (~110°C) the observed T_1 frequency dependence is quite large and only semiquantitatively accounted for using this modified theory. The ramifications of multifrequency experiments with respect to the proper interpretation of complex motions are explored. ←

approximately 1 page about

17. KEY WORDS AND DOCUMENT ANALYSIS		
a. DESCRIPTORS	b. IDENTIFIERS/OPEN ENDED TERMS	c. COSATI Field/Group

18. DISTRIBUTION STATEMENT	19. SECURITY CLASS (This Report)	21. NO. OF PAGES
RELEASE TO PUBLIC	UNCLASSIFIED	18
	20. SECURITY CLASS (This page) UNCLASSIFIED	22. PRICE

EPA Form 2220-1 (9-73)

EPA-600/J-78-194
Journal Article
PB82-155243

[Reprinted from the Journal of the American Chemical Society, 100, 410 (1978).]

Interpretation of Complex Molecular Motions in Solution. A Variable Frequency Carbon-13 Relaxation Study of Chain Segmental Motions in Poly(*n*-alkyl methacrylates)

George C. Levy, David E. Axelson, Robert Schwartz, and Jiri Hochmann

REPRODUCED BY
NATIONAL TECHNICAL
INFORMATION SERVICE
U.S. DEPARTMENT OF COMMERCE
SPRINGFIELD, VA 22161

Interpretation of Complex Molecular Motions in Solution. A Variable Frequency Carbon-13 Relaxation Study of Chain Segmental Motions in Poly(*n*-alkyl methacrylates)

George C. Levy,*[1] David E. Axelson,* Robert Schwartz, and Jiri Hochmann

Contribution from the Department of Chemistry, Florida State University, Tallahassee, Florida 32306. *Received May 11, 1977*

Abstract: An extensive variable temperature study of poly(*n*-butyl methacrylate) and poly(*n*-hexyl methacrylate) at two widely separated frequencies (67.9 and 22.6 MHz) has revealed that a model requiring a nonexponential autocorrelation function, or, its mathematical equivalent, a distribution of correlation times, describes the NMR parameters obtained for the backbone carbons. However, frequency-dependent spin–lattice relaxation time (T_1) and nuclear Overhauser effect (NOE) behavior observed for all side-chain carbons, including the terminal methyls, with NT_1s of the order of 20 s, could not be described in terms of present theoretical approaches. A new model developed retains the distribution of correlation times for the backbone carbons and incorporates the effects of multiple internal rotations about the carbon–carbon single bonds for the side-chain carbons. This model predicts a substantial frequency dependence for broad distribution widths which can quantitatively reproduce almost all of the observed data. For the highest temperatures attained (~110 °C) the observed T_1 frequency dependence is quite large and only semiquantitatively accounted for using this modified theory. The ramifications of multifrequency experiments with respect to the proper interpretation of complex motions are explored.

Introduction

As equipment and relaxation measurement techniques have become more sophisticated and sensitive in the last few years, the amount of molecular dynamics information which can be obtained by NMR has increased greatly.[2-5] However, as these experiments become more accurate, the possibility of elucidation of more subtle molecular dynamic processes is enhanced. These additional consequences of the development of the field result in other problems, namely, the analysis of any relaxation data presupposes that an adequate model has been chosen. The generally accepted approximation of a single correlation time characterizing the exponential decay of the autocorrelation function has been the choice of preference for most analyses.[6-13]

Theoretical advances[14-23] have allowed for the interpretation of more complex molecular motions but extensive variable temperature and variable frequency experiments have not been available to properly test the various models. Such testing should encompass measurement of all three accessible parameters, the spin–lattice relaxation time, T_1, the spin–spin relaxation time, T_2, and the nuclear Overhauser enhancement, NOE. However, the more stringent experimental requirements

0002-7863/78/1500-0410$01.00/0

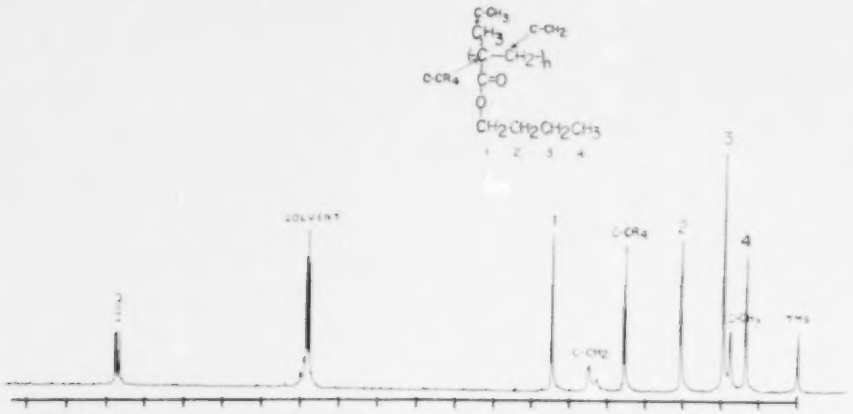

Figure 1. Proton-decoupled ^{13}C NMR spectrum of a 50% (w/w) solution of poly(*n*-butyl methacrylate) in toluene-d_8. Spectrum obtained at 40 °C and 67.9 MHz.

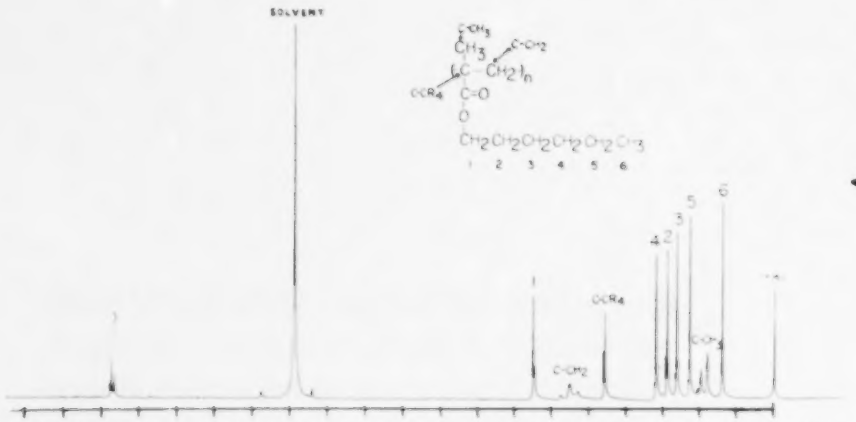

Figure 2. Proton-decoupled ^{13}C NMR spectrum of a 50% (w/w) solution of poly(*n*-hexyl methacrylate) in benzene-d_6. Spectrum obtained at 40 °C and 67.9 MHz.

associated with accurate T_2 measurements negate the detailed use of this parameter in the present study. Line broadening due to the effects of tacticity further complicate such measurements.

We wish to report the results of an extensive ^{13}C NMR relaxation study of two polymers, poly(*n*-butyl methacrylate) and poly(*n*-hexyl methacrylate), at a number of temperatures and at two widely different magnetic fields. The inadequacies of the available models will be discussed and suggestions for improvement of the present theories will be proposed.

Experimental Section

Poly(*n*-butyl methacrylate) (PBMA) was obtained from Polyscience, Inc., as a high molecular weight material. Solutions were made without further purification using toluene-d_8 and benzene-d_6 as solvents. Poly(*n*-hexyl methacrylate) (PHMA) was purchased as a toluene solution (25 wt %) from the Aldrich Chemical Co. All samples were sealed in NMR tubes but not degassed. PHMA samples (50% w/w) were prepared by solute concentration at ~70°C under a N_2 gas stream.

Natural abundance ^{13}C spectra were obtained using Bruker HX-270 and HFX-90 spectrometers operating for ^{13}C at 67.9 and 22.6 MHz, respectively. Representative spectra are shown in Figures 1 and 2. Free induction decays were accumulated using Nicolet 1080 series computers and Fourier transformed to yield 4096 data points in the frequency domain spectra. Quadrature detection was employed for all T_1 experiments and some of the NOE determinations.

T_1 measurements were performed using the (T-180°-t-90°), fast inversion recovery pulse sequence, FIRFT.[24] Intensities obtained from the FIRFT spectra were used to calculate relaxation times using the expression $\ln(A_\infty - A_t) = t/T_1$ where A_∞ is the equilibrium amplitude of the fully relaxed peak and A_t is the amplitude of the peak at some pulse delay time t. The estimated error in T_1 is approximately 10% but repetitive measurements indicated that the reproducibility was usually much better. A typical set of experimental results is shown in Figure 3.

Nuclear Overhauser enhancement factors (NOEFs) were determined with gated decoupling[25] generally using single-phase detection. Experiments were set up to take two sets of spectra: two spectra were acquired with constant wide-band decoupling and two others using gated decoupling. The pulse interval equaled or exceeded *ten times the longest T_1 involved*. NOE values were determined from the average of the two data sets and are considered accurate to within ±15–20%.

The temperature was controlled with a Bruker B-ST100 heating unit. The sample temperature was measured using a thermometer placed in an equivalent sample tube containing an equivalent volume of benzene or toluene solvent, under identical decoupling conditions. Decoupling power was kept low to prevent differential sample temperatures during gated decoupling NOE measurements (~3–4 W).

All theoretical calculations were performed on a CDC 6400 computer with programs written in FORTRAN IV.

Theory

For two nonequivalent spin-½ nuclei the spin–lattice relaxation time[6,7] and the nuclear Overhauser enhancement factor may be written in terms of the spectral density functions, $J_i(\omega)$, as

$$\frac{1}{T_1} = 0.1N\gamma_C{}^2\gamma_H{}^2\hbar^2 r^{-6}[J_0(\omega_H - \omega_C) + 3J_1(\omega_C) + 6J_2(\omega_H + \omega_C)] \quad (1)$$

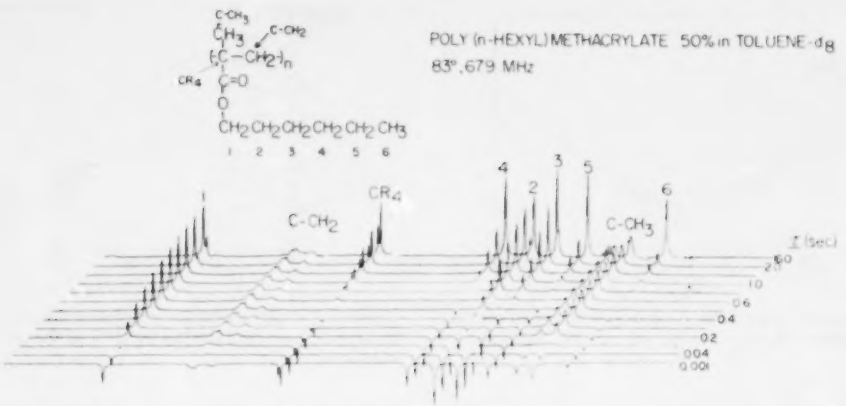

Figure 3. Proton-decoupled ^{13}C NMR spectra of a 50% (w/w) solution of poly(*n*-hexyl methacrylate) in toluene-d_8. The number to the right of each spectrum is τ, the interval between the 180° and the 90° pulse in the FIRFT sequence, and is given in seconds. The equilibrium spectrum is shown at the top while the others are partially relaxed spectra.

and

$$\text{NOEF (NOE-1)} = \eta = 3.976\left[\frac{6J_2(\omega_H + \omega_C) - J_0(\omega_H - \omega_C)}{J_0(\omega_H - \omega_C) + 3J_1(\omega_C) + 6J_2(\omega_H + \omega_C)}\right] \quad (2)$$

where N is the number of directly attached hydrogens (for ^{13}C-^1H dipolar relaxation), γ_C and γ_H are the magnetogyric ratios of carbon and hydrogen, respectively, and r is the carbon–hydrogen internuclear distance.

If the autocorrelation function can be described by an exponential characterized by a single correlation time,[6] τ_c, one obtains

$$J_i(\omega) = \frac{\tau_c}{1 + \omega^2\tau_c^2} \quad (3)$$

For a distribution of correlation times[26-31] (mathematically indistinguishable[26] from nonexponential autocorrelation functions) one can introduce a multiplicative factor known as the probability density function, $G(\tau_c)$,[26] and eq 3 becomes

$$J_i(\omega) = \int_0^\infty \frac{G(\tau_c)\tau_c}{1 + \omega^2\tau_c^2}\,d\tau_c \quad (4)$$

where

$$\int_0^\infty G(\tau_c)d\tau_c = 1 \quad (5)$$

Of the many possible distribution functions[26-32] only the spectral densities for three (Cole–Cole,[27,29] Monnerie diamond lattice,[29] and log $-\chi^2$ [28,29]) and their derivatives will be discussed.

Each distribution has been found to yield quantitatively similar results when applied to a common data set, especially if the experimental data are obtained at a single field.[29] Under these circumstances, choosing the model which best describes polymeric dynamics is somewhat arbitrary. The pros and cons of these three functions will be briefly discussed below. It is important, however, to examine the general consequences of adopting this type of model for the behavior of the backbone carbon molecular dynamics. Many of the trends experimentally determined for polymer side-chain carbons are intimately linked to the model chosen for the backbone carbons.

Invocation of a distribution results in the prediction of frequency-dependent relaxation times over a very wide range of correlation times, *including* within the so-called extreme narrowing region predicted from a single correlation time model.[26-29] Thus, very long relaxation times *can* be field dependent. Measurements made (and conclusions drawn) in such cases may be quite misleading if only one magnetic field is used to obtain the T_1 data. As shown in Figure 5, NOEs also exhibit more complex behavior relative to that predicted from single correlation time models. A decrease in the NOE can be observed at shorter correlation times, while an increase in the NOE is obtained at longer correlation times, both depending on the width of the distribution.[28,29] Therefore, carbons exhibiting long, but still frequency-dependent, T_1s may have unexpectedly low NOEs. Conversely, carbons with very long correlation times may have abnormally high NOEs.

The position of the T_1 minimum for a given carbon as a function of motion (temperature) is also affected by the width of the distribution of correlation times, especially for broader distributions (as in the log $-\chi^2$ model).[28] In addition, the curves for T_1 and NOE as a function of correlation time become more shallow as the width of the distribution increases. This is illustrated in Figures 4 and 5 for the log $-\chi^2$ distribution. As a result (for a constant distribution width) the observed temperature dependence of the T_1s and NOEs may be small, particularly for very broad distributions. For (probably common) cases in which the distribution width varies with temperature the derivation of a "simple" activation energy for the polymer thus becomes impossible.[33]

The spectral densities for the models investigated in detail will now be discussed briefly.

Log $-\chi^2$ Distribution. The spectral density function for the log $-\chi^2$ distribution[28,29] is given by

$$J_i(\omega) = \int_0^\infty \frac{\bar{\tau}H(s)(\exp_b s - 1)}{(b-1)\{1 + \omega^2\bar{\tau}^2[(\exp_b s - 1)/(b-1)]^2\}}\,ds \quad (6)$$

where

$$H(s) = \frac{1}{\Gamma(p)}(ps)^{p-1}e^{-ps}p \quad (7)$$

In eq 7 p is the width parameter and $\Gamma(p)$ (which is a normalization factor) is the value of the Γ function for the value p.

Owing to the use of a logarithmic scale the variable s is defined by

$$s = \log_b[1 + (b-1)\tau_c/\bar{\tau}] \quad (8)$$

The average correlation time is given by $\bar{\tau}$ and the logarithmic base is described by the parameter b (usually taken to be 1000). For p greater than 100 this model reduces to the single correlation time model. Note that this is an asymmetric distribution with greater weighting of the correlation times *for longer* τ *values*.[28]

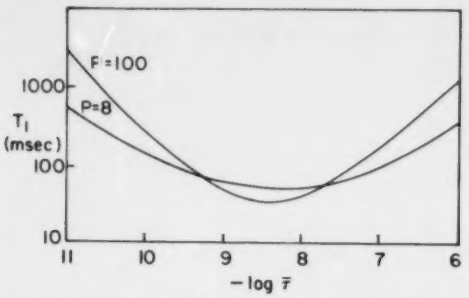

Figure 4. Spin-lattice relaxation time, T_1, as a function of correlation time, $\bar{\tau}$, and distribution width, p, for the log $-\chi^2$ distribution (22.6 MHz).

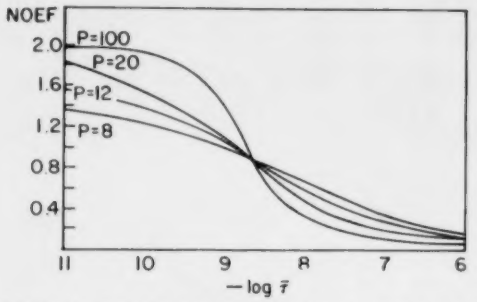

Figure 5. Nuclear Overhauser enhancement factor, NOEF, as a function of correlation time and distribution width for the log $-\chi^2$ distribution (22.6 MHz).

Log $-\chi^2$ Distribution Including "Simple" Internal Rotation.[29] The first modification to be made involves inclusion of internal rotation in the equations, in anticipation that such a correction may better describe the motion of polymer side chains. The internal motion is incorporated under the following assumptions: (1) only one extra degree of freedom is involved and (2) the carbon in question is assumed to experience a threefold barrier to rotation. In addition, it can be assumed that the motion of the substituent is either dependent on or independent of the motion of the backbone.

The spectral densities for the dependent case are

$$J_i(\omega) = \int_0^\infty H(s)\left[\frac{1}{4}(1 - 3\cos^2\alpha)^2 \frac{\bar{\tau}\left(\frac{b^s - 1}{b - 1}\right)}{1 + \omega^2\bar{\tau}^2\left(\frac{b^s - 1}{b - 1}\right)^2} + 3(\sin^2 2\alpha + \sin^4\alpha) \times \frac{\left(\frac{2K}{2K + 3}\right)\bar{\tau}\left(\frac{b^s - 1}{b - 1}\right)}{1 + \omega^2\left(\frac{2K}{2K + 3}\right)^2\bar{\tau}^2\left(\frac{b^s - 1}{b - 1}\right)^2}\right]ds \quad (9)$$

where $K = \tau_g/\tau_c$, τ_g is the correlation time for internal rotation, and α is the angle between the CH vector and the rotation axis. It is anticipated that this formulation would be most successful for describing the motion of methyl groups directly attached to the polymer backbone.

Log $-\chi^2$ Distribution Including Multiple Internal Rotations. The final change involves incorporating multiple internal rotations into the dynamics of the side-chain carbons while maintaining the distribution of correlation times for the backbone carbons.

The theory behind derivation of spectral density functions for multiple internal rotations has been described in previous papers[18-20] and only the essential equations relevant to the present discussion will be given here.

The spectral density functions for internal rotation alone are given by[18-20]

$$J_i(\omega) = \sum_{a,b,\ldots,i} |d_{ab}(\beta_a)|^2 |d_{bc}(\beta_b)|^2 \ldots |d_{ni}(\beta_n)|^2 \times |d_{io}(\beta_i)|^2 \frac{\tau}{1 + \omega^2\tau^2} \quad (10)$$

where

$$\tau = (6D_o + a^2D_a + b^2D_b + \ldots + i^2D_i)^{-1} \quad (11)$$

and D_o is the overall (isotropic) rotational diffusion constant for the molecule, D_a, D_b, . . . , D_i are the rotational diffusion constants for the carbon–carbon bonds in the alkyl chain, and the d_{ij} are the reduced second-order Wigner rotation matrices. The angles, β_a, β_b, . . . , are the angles between successive axes of rotation and β_i is the angle between the final axis of rotation and the dipole–dipole vector between the coupled nuclei under investigation.

London and Avitabile[20] have shown that the problem may be considerably simplified, the resulting spectral densities being given by

$$J_i(\omega) = \sum_{a,b,\ldots,i} B_{ab}B_{bc}\ldots B_{hi}B_{io}\frac{\tau}{1 + \omega^2\tau^2} \quad (12)$$

where the B matrix elements are geometric factors describing the alkyl chain (their values can be found in ref 20). Rather than refer to these papers individually, the above theory of multiple internal rotations developed by Wallach,[17] Levine[18,19] et al., and London[20] et al. will be referred to collectively as the WLL theory.

We propose that the WLL-derived theory may be unsatisfactory for describing the frequency-dependent dynamic parameters (T_1, NOE) of side-chain carbons attached to "macromolecules" whose overall molecular motion must be described by a distribution of correlation times.[34] The extensive data obtained in the present work allow a rigorous comparison of these theories to be made.

To adequately explain the two field T_1 and NOE data we have extended the present WLL theory to the situation including a distribution of correlation times for the backbone carbons. This is accomplished by applying the probability density function for the log $-\chi^2$ distribution (eq 7) to the spectral density given in eq 10

$$J_i(\omega) = \sum_{a,b,\ldots,i} |d_{ab}(\beta_a)|^2 \ldots |d_{hi}(\beta_h)|^2 |d_{io}(\beta_i)|^2 \times \int_0^\infty \frac{\frac{1}{\Gamma(p)}(ps)^{p-1}e^{-ps}p\,(\exp_b s - 1)\tau^* ds}{|b - 1|\{1 + \omega^2\tau^{*2}[|\exp_b s - 1|/(b - 1)]^2\}}$$

where

$$\tau^* = (6D_o^* + a^2D_a + b^2D_b + \ldots + i^2D_i)^{-1} \quad (13)$$

and

$$D_o^* = \left(\frac{1}{6\tau_o}\right)\left(\frac{b - 1}{b^s - 1}\right)$$

(The parameter b in the log $-\chi^2$ distribution formulation was taken to be 1000. This should not be confused with the dummy variable b used in the summation over the rotation matrices.) A corresponding expression which is computationally faster may be derived by applying the appropriate probability density function to eq 12. This latter formulation was used in the present case.

Of the possible choices of distributions upon which one could expand the model for side-chain dynamics, the log $-\chi^2$ dis-

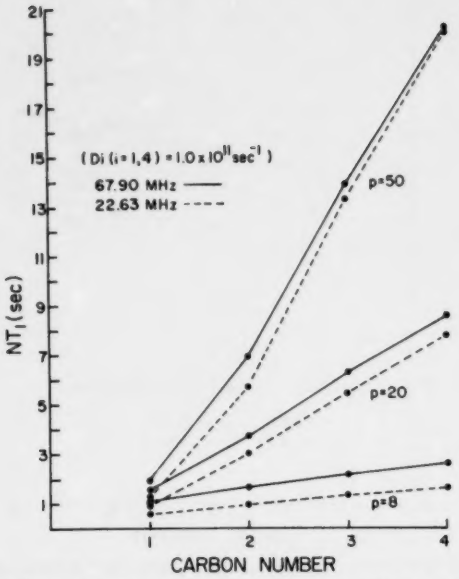

Figure 6. Spin-lattice relaxation times for side-chain carbons as a function of distribution width. The diffusion constants equal along the chain with values $D_i = 1.0 \times 10^{11}$ s^{-1} for 67.905 (—) and 22.635 MHz (- - - -). Backbone (carbons) isotropic correlation time is $1. \times 10^{-10}$ s.

tribution model[28] was chosen. All of the models suffer from various deficiencies. The Cole–Cole[27,29] is a symmetrical distribution while the asymmetrical log $-\chi^2$ model favorably weights the longer correlation times to be expected in polymeric systems. It should be noted that there is no particular advantage in using the asymmetric log $-\chi^2$ distribution for systems characterized by relatively narrow distributions. It can be shown[35] that the χ^2 distribution can be approximated very closely by a normal (i.e., symmetric) distribution for cases in which the number of degrees of freedom is approximately 45 or greater. The most serious deficiency of the Monnerie diamond lattice model is the erratic temperature dependence of τ_D/τ_0 for comparable polymers. Also, the physical basis of the model has been questioned.[29a] To further complicate the situation Heatley and Cox[29b] have determined that the most consistently successful interpretation of the polymer motion in poly(vinyl acetate) in solution (as determined by ^{1}H NMR) requires the conformational jump (Monnerie) model. The log $-\chi^2$ model suffers from the presence of the parameter b which must be judiciously chosen so that a wide range of data can be examined with a change in the width parameter, p, only. The model breaks down for cases in which $p < \ln b$.

Levine et al.[18,19] have shown that the decay of the autocorrelation function for carbons more than five bonds removed from a motional restriction, such as that imposed by a "macromolecule", is not affected by varying the diffusion constant of the macromolecule. Thus the T_1's of those carbons were predicted to be independent of the motion of the macromolecule. Levine[36] noted that such calculations ignore steric hindrance and conformational interdependences along such a chain. He suggested a more realistic model which incorporated a Monte Carlo approach to the calculation of the time evolution of allowed conformations and an appropriate statistical transition matrix to determine the probabilities of conformational changes. A particularly strong correlation in motions for pairs of adjacent C–H vectors along a chain can be induced (theoretically) by an appropriate choice of the parameter describing the population ratio of the allowed conformations, in conjunction with the introduction of forbidden conformations. This correlation exists for at least the first six pairs of C–H vectors assuming that the potential energy well profiles for different chain segments are not perturbed by differential intermolecular interactions of significance.

Thus the possibility of long-range ordering of molecular motions is not excluded from the WLL theory. Rather the facts point more to the conclusion that these long-range "cooperative" motions have merely eluded detection. This *emphasizes* the need for multifrequency T_1 and NOE measurements for accurate interpretation of dynamics in polymeric and other complex molecular systems.

Recently, Yasukawa et al.[37] have simulated the random motions of an *n*-hexyl chain bound to a macromolecule [poly(*n*-hexyl-4-vinylpyridinium bromide)] by Monte Carlo methods. Different models were tested according to the transition probabilities chosen for the conformational interconversions. They found that the spectral density functions for the main chain agreed well with the conventional spectral density approximation $[2\tau/(1 + \omega^2\tau_c^2)]$ but that the functions for the hexyl chain could not be represented by the same expression. While a satisfactory fit to the experimental T_1 values was obtained, no mention was made of the predictive value of the theory as applied to the NOEs or to changes in frequency.

Calculations. Numerical Results

Figure 6 illustrates the trends exhibited for the various carbons of an alkyl chain which is described by equal internal rotational diffusion constants ($D_i = 1.0 \times 10^{11}$ s^{-1}) about each bond, the chain being attached to a "macromolecule" (defined as carbon 0) with an effectively isotropic correlation time of 1.0×10^{-10} s.

When the overall molecular correlation time ($\bar{\tau}_{mol}$) is longer than the correlation time for internal rotation the relaxation times increase dramatically along the chain (subject, in this case, to the D_is being constant along the chain). However, the relative NT_1 differentials for these carbons are attenuated considerably by the presence of a distribution of correlation times for the backbone carbons, until finally for a broad distribution (e.g., $p = 8$) the NT_1's change very little over the length of the chain. The same effect occurs when the internal rotational diffusion constant is slower than the overall motion.[38] The presence of a distribution can be distinguished from this latter situation by the frequency dependence of the T_1s, as well as from certain trends in the NOEFs (vide infra).

There is only a slight frequency dependence for the T_1s near the end of the chain with a narrow distribution ($p = 50$). The frequency dependence increases considerably for broader distributions and is present *even* for the end methyls of long chains when p is $\lesssim 10$. As the trends (Figure 6) indicate, the frequency dependence may disappear entirely for side-chain carbons attached to a backbone whose motion can be described by a single correlation time model. The presence of the distribution lowers T_1s for the side-chain carbons relative to the values calculated for the single correlation time model for identical diffusion constants. Also apparent is the fact that a change in the width of the distribution can induce a large change in the T_1s.

Figure 7 illustrates the effects on the nuclear Overhauser enhancement factor assuming the parameters given in Figure 6. The NOEFs range from 1.2 to 1.5 for C-1 under the given conditions at both fields and increase for the remaining carbons in the chain. For these latter carbons, however, when $p \gtrsim 50$ the NOEF is substantial and might be considered maximized within experimental error (depending on the accuracy of the experiment). For very broad distributions these NOEF values are quite low, even for C-4 having a value of approximately 1.4. With most distribution widths, there is only a slight frequency dependence of the NOEF for the side-chain carbons.

Another possible situation is depicted by Figures 8 and 9. The rotational diffusion constants along the chain have been

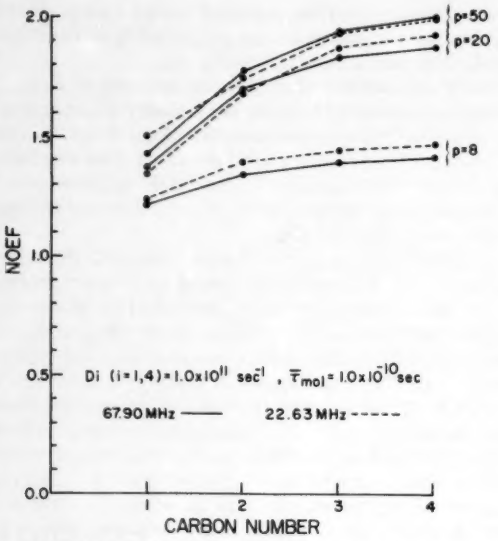

Figure 7. Nuclear Overhauser enhancement factors for side-chain carbons as a function of distribution width. Conditions are given in Figure 6 caption.

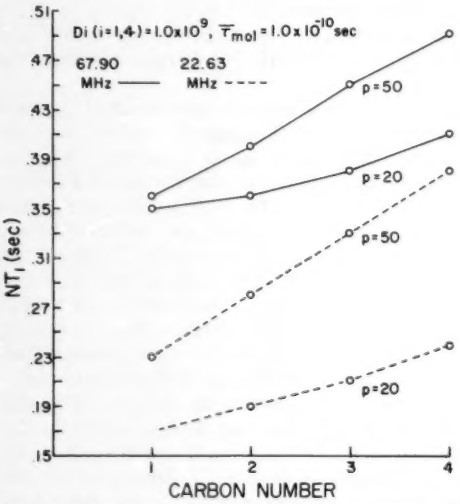

Figure 8. Spin–lattice relaxation times of side-chain carbons as a function of distribution width. All diffusion constants are equal along the chain with a value of $D_i = 1 \times 10^9\ s^{-1}$ for 67.905 (—) and 22.635 MHz (- - - - -). Backbone (carbons) isotropic correlation time is $1. \times 10^{-10}$ s.

reduced by two orders of magnitude so that the internal motion is now comparable to the overall or polymer backbone segmental molecular motion. As has been noted and as shown in Figure 8 there is only a small gradation in the relaxation times along the side chain (note the change in scale of T_1 values). When internal motions are much slower than the overall molecular motion there would be virtually no change in the T_1s along the chain. In this case there is a *substantial frequency dependence* which, as expected, increases for the broader distribution. (When τ_{int} ($\tau_{int} = (6D_i)^{-1}$) is longer than τ_{mol} the relative frequency dependence of the T_1s is greater than for the case τ_{int} less than τ_{mol}.)

The effects of these motional parameters on the NOEFs are substantial (Figure 9). Slower motion results in a larger frequency dependence than for $D_i = 1.0 \times 10^{11}$. Also, the leveling effect of the distribution causes the NOEFs to be substantially lower. For $p = 20$ the C-4 carbon NOEF is 1.2–1.4 at the two

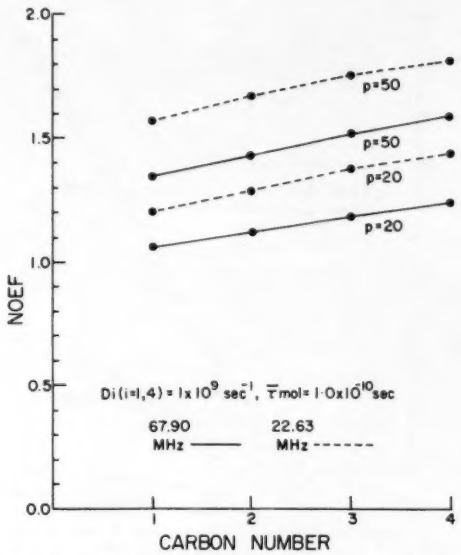

Figure 9. Nuclear Overhauser exhancement factors for side-chain carbons as a function of distribution width. Conditions the same as for Figure 8.

fields, whereas for $D_i = 1.0 \times 10^{11}\ s^{-1}$ a much broader distribution ($p = 8$) was required to attain comparable NOEF values. The effect of the distribution width is enhanced also. Changing from $p = 20$ to $p = 50$ for $D_i = 1.0 \times 10^9\ s^{-1}$ results in an NOEF change of 0.35 for C-4; the same change in p when $D_i = 1.0 \times 10^{11}\ s^{-1}$ affects the NOEF for C-4 by only 0.1.

It should be noted that the model invoked is logically extended from one carbon to the next. Determination of the average backbone correlation time, $\bar{\tau}$, provides the basis for calculation of the side-chain carbon data. The rotational diffusion constant for the first "effective" carbon–carbon bond is varied until the best fit for the two field data is obtained. Keeping this value constant, the data for the next carbon are reproduced by varying the next rotational diffusion constant. The process is repeated as often as necessary to describe the entire side chain.

Multiple Field Measurements. Heatley and Begum[29] noted that the motional parameters for a theory should be dependent on observable parameters if the former are to be calculated with accuracy. The areas which are least sensitive, in general, are the regions of the T_1 minimum and the long correlation time region for the NOEF. In these cases the experimental data (within the limits imposed also by experimental accuracy) may therefore be reproduced by a number of *different* model parameters. This ambiguity is alleviated by the use of two magnetic fields as *widely separated as possible*. Three (or more) field strengths would be even more advantageous. Figure 10 illustrates that a single frequency measurement of T_1 can lead to the prediction that any distribution width (up to and including the possibility that no distribution exists) will reproduce the experimental T_1 for certain correlation times. The possible need for invocation of a complex form for the autocorrelation function clearly cannot always be properly evaluated from data obtained at one frequency (for one nuclide, at one magnetic field).

Results and Discussion

Examination of the T_1 data for PBMA and PHMA (Tables I–VI) reveals several characteristic trends. The T_1s for the side-chain carbons generally increase as a function of distance from the backbone. This is not unexpected, since similar behavior is observed in smaller molecular systems having ali-

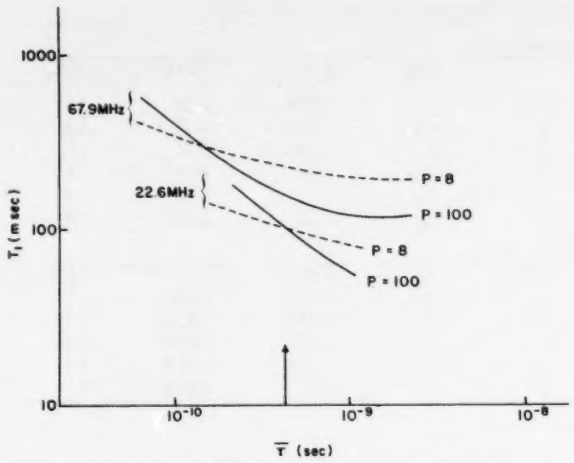

Figure 10. Spin–lattice relaxation time vs. correlation time for distribution widths of $p = 8$ (- - - -) and $p = 100$ (—) for 67.905 and 22.635 MHz.

Table I. ^{13}C Spin–Lattice Relaxation Times of Poly(*n*-butyl methacrylate) in 50% (w/w) Solution in Toluene-d_8

Temp, °C	C-1	C-2	C-3	C-4	CCH_3	CCH_2	CCR_4
			T_1 (67.9 MHz), s				
−5	0.27	0.20	0.35	0.93	0.053	*a*	2.7
6	0.35	0.23	0.39	1.0	0.057	0.21	2.3
21	0.35	0.37	0.73	1.7	0.062	0.17	2.3
46	0.33	0.57	1.2	2.4	0.081	0.12	1.8
55	0.33	0.69	1.5	2.9	0.11	0.098	1.7
75	0.28	0.79	1.5	3.4	0.15	0.085	1.5
80	0.29	0.90	2.5	3.8	0.14	0.086	1.4
93	0.31	0.95	2.7	4.0	0.18	0.093	1.3
98	0.32	1.1	2.8	4.3	0.18	0.094	1.5
111	0.35	1.4	3.4	6.2	0.26	0.11	1.6
			T_1 (22.6 MHz), s				
10	0.13	0.20	0.45	1.1	0.025	*a*	0.69
22	0.11	0.25	0.52	1.3	0.030	0.034	0.64
37	0.093	0.27	0.70	1.5	0.033	0.031	0.56
49	0.094	0.33	0.89	1.7	0.048	0.031	0.54
66	0.085	0.37	0.95	1.8	0.059	0.030	0.49
83	0.10	0.45	1.1	2.1	0.079	0.035	0.53
105	0.15	0.67	1.4	2.8	0.13	0.043	0.70

[a] Not evaluated.

phatic chains effectively anchored at one end by the presence of a relatively immobile functional group or because of ionic or bonding interactions between the molecule and its immediate environment.[3,5,13,19,39,40] In the absence of such a situation NT_1 values generally increase from the center of mass.[19,40-42] Since motional restriction is greater for the carbon positions closer to the restricting group, correlation times describing these positions should be longer than for carbons removed from the site of restriction. The motions along the aliphatic side chains of PBMA and PHMA are predominantly characterized by apparent correlation times to the left of the T_1 minimum. Note, however, that the T_1 values for C-2 sometimes show a slight decrease with respect to the T_1 values for C-1 and C-3 (at lower temperatures and at the higher field strength).

The most surprising fact is that there is a consistently large field dependence associated with the T_1s for all of the side-chain carbons. Simple theory[6-8] predicts that the dipolar T_1 of a carbon is *independent* of the magnetic field strength if the correlation time describing its motion is within the extreme narrowing region $[(\omega_C + \omega_H)^2\tau_c^2 \ll 1]$.

Table II. Nuclear Overhauser Enhancement Factors for Poly(*n*-butyl methacrylate) in 50% (w/w) Solution in Toluene-d_8

Temp, °C	C-1	C-2	C-3[c]	C-4	CCH_3	CCH_2	CCR_4
			NOEF (67.9 MHz), η[a]				
−5	2.0	1.9		2.0	*b*	*b*	0.51
14	1.4	1.7		1.8	0.71	0.67	0.47
34	0.81	1.6		1.6	0.83	0.56	0.61
42	1.1	1.6		1.5	1.2	0.43	0.66
52	0.80	1.4		1.5	1.2	0.44	0.50
64	0.61	1.3		1.4	1.3	0.44	0.59
80	0.54	1.3		1.3	1.3	0.43	0.56
101	0.42	0.98		1.3	1.4	0.36	0.59
			NOEF (22.6 MHz), η[a]				
11	0.47	1.5		1.6	0.99	*b*	0.89
21	0.54	1.7		1.7	*b*	0.30	0.88
31	0.23	1.0		1.2	0.91	0.30	*b*
50	0.69	1.2		1.6	1.8	0.40	0.68
63	0.79	1.9		1.3	1.3	0.71	0.75
81	0.9	1.1		1.4	1.8	0.66	1.3
104	1.1	1.3		1.4	1.4	0.59	1.1

[a] NOE = NOEF + 1; $NOEF_{max} = 1.99$; estimated maximum error ±10%. [b] Not evaluated. [c] Not evaluated due to overlap with solvent resonance.

With the exception of C-1, for each side-chain carbon an increase in temperature results in an increase in T_1. The C-1 T_1 values remain relatively constant over the wide temperature range studied (~100 °C). There is evidence for a shallow T_1 minimum for C-1 in PBMA and PHMA at the lower field.

As the temperature is increased the backbone methylene carbon in PBMA shows a definite T_1 minimum at both magnetic fields while the backbone CH_2 carbon of PHMA monotonically decreases over the same range. Differences may originate from the fact that, for comparable temperatures, PHMA is further above its glass transition temperature[48] and hence has relatively more freedom of motion.

The minima observed for PBMA (50% w/w in toluene-d_8) also prove interesting. From plots of the data the backbone CH_2 T_1 minimum is found at ca. 56 °C at 22.6 MHz but at ca. 77 °C at 67.9 MHz. This is consistent with the fact that the T_1 minimum for the 67.9-MHz magnetic field strength occurs for a shorter correlation time than at the 22.6-MHz strength. This implies that a greater temperature would be required to observe the T_1 minimum at even higher field strengths. The same trend is observed for the quaternary backbone carbon of PBMA.

A minimum is observed for PHMA (50% w/w in toluene-d_8, Table III) at 22.6 MHz only, the higher field strength requiring temperatures that are unattainable in toluene-d_8. A more dilute solution of PHMA (20% w/w in toluene-d_8) where the polymer is somewhat more mobile does exhibit a minimum at approximately 50 °C (Table VI). The observed T_1 minimum for CCH_2 is also consistent with a higher p value than that observed for the more concentrated solution.

Table II contains the nuclear Overhauser enhancement factors for PBMA. At low temperatures the NOEFs determined at 67.9 MHz for the side-chain carbons tend to equalize in magnitude near the theoretical maximum value of 2. As the temperature is increased the NOEF for C-1 decreases considerably (by a factor of ca. 5) while the C-2 and C-4 NOEF values decrease at a less drastic rate (by a factor of ca. 2). The high-field NOEF differential between C-1 and C-2 increases as the temperature increases while the C-2 and C-4 differential remains relatively constant. The backbone methylene NOEF also decreases somewhat with temperature at 101 °C reaching an NOEF which is comparable to that observed for C-1 of the side chain. The backbone methyl substituent NOEF increases with temperature by a factor of 2 over the range 14–101 °C.

Table III. ^{13}C Spin–Lattice Relaxation Times of Poly(*n*-hexyl methacrylate) in 50% (w/w) Solution in Toluene-d_8

Temp, °C	T_1 (67.9 MHz), s								
	C-1	C-2	C-3	C-4	C-5	C-6	CCH_3	CCH_2	CCR_4
3	0.32	0.21	0.30	0.57	0.81	1.5	0.069	0.32	2.9
34	0.30	0.30	0.55	1.1	1.7	2.6	0.068	0.13	1.8
49	0.31	0.47	0.85	1.6	2.4	3.7	0.092	0.11	1.6
63	0.31	0.54	1.1	2.1	3.2	4.6	0.10	0.097	1.6
83	0.30	0.65	1.4	2.3	3.7	5.3	0.12	0.090	1.5
100	0.31	0.81	1.8	2.9	5.1	7.1	0.22	0.093	1.4
	T_1 (22.6 MHz), s								
17	0.12	0.14	0.26	0.47	0.75	1.6	0.024	*a*	0.63
43	0.11	0.24	0.47	0.90	1.5	2.3	0.037	0.035	0.54
64	0.10	0.28	0.63	1.1	2.1	3.3	0.057	0.029	0.40
74	0.098	0.36	0.83	1.5	2.5	4.2	0.073	0.028	0.46
89	0.10	0.38	0.95	1.7	3.0	4.8	0.086	0.030	0.47
102	0.13	0.52	1.0	1.8	3.3	5.1	0.14	0.042	0.58

[a] Not evaluated.

Table IV. Nuclear Overhauser Enhancement Factors for Poly(*n*-hexyl methacrylate) in 50% (w/w) Solution in Toluene-d_8

Temp, °C	NOEF (67.9 MHz), η[a]								
	C-1	C-2	C-3	C-4	C-5	C-6	CCH_3	CCH_2	CCR_4
3	2.1	1.9	1.7	1.6	1.5	1.6	0.7		1.1
17	1.7	1.8	1.6	1.6	1.5	1.7	0.8	0.7	0.8
35	1.2	1.6	1.7	1.6	1.6	1.7	1.1	0.6	0.5
50	1.0	1.6	1.7	1.8	1.8	1.7	1.1	0.3	0.6
66	1.9	1.6	1.8	1.8	1.8	1.8	1.7	0.6	0.7
83	1.9	1.5	1.8	1.8	1.9	1.9	1.6	0.4	0.6
100	1.8	1.5	1.8	1.9	1.9	2.0	1.8	0.5	0.7
	NOEF (22.6 MHz), η[a]								
17	0.6	1.7	1.8	1.6	1.9	2.0	0.9	0.4	0.5
44	0.9	1.6	1.7	1.7	1.7	1.8	1.1	0.3	0.9
66	1.1	1.5	1.3	1.2	1.1	1.3	1.5	0.5	0.6
76	0.9	1.3	1.4	1.3	1.5	1.4	1.0	0.6	0.7
90	0.9	1.1	1.1	1.4	1.2	1.4	1.1	0.9	0.8
103	1.1	1.3	1.3	1.5	1.2	1.2	1.6	0.5	0.8

[a] NOEFs ±5–15%.

Table V. ^{13}C Spin–Lattice Relaxation Times of Poly(*n*-butyl methacrylate) in 50% (w/w) Solution in Benzene-d_6

Temp, °C	T_1 (67.9 MHz), s						
	C-1	C-2	C-3	C-4	CCH_3	CCH_2	CCR_4
10	0.4	0.30	0.51	1.2	0.065	*a*	2.5
22	0.39	0.38	0.67	1.7	0.069	0.19	2.3
31	0.46	0.51	1.0	2.3	0.076	0.17	2.4
40	0.41	0.53	1.1	2.4	0.078	0.13	2.1
50	0.26	0.65	1.4	2.7	0.088	0.11	1.9

[a] Not evaluated.

The situation is somewhat different for the low-field data. The C-1 NOEF *increases* with temperature while the C-2 and C-4 NOEF values remain relatively constant over the temperature range, but at lower than the maximum permissible value. At high temperatures the 22.6-MHz NOEFs for the side-chain carbons tend to equalize. A small increase in NOEF with temperature is noted for both of the backbone carbons.

Table IV contains the PHMA nuclear Overhauser enhancement factors. The trends are comparable in general with those delineated for PBMA, although the NOEFs for C-1 at 67.9 MHz above 50 °C are quite large compared with the values found in PBMA.[49]

Main-Chain Carbons. Table VII gives the results of the calculation of the distribution widths and correlation times for PBMA over a wide range of temperatures. The virtual insensitivity of the main chain T_1 and NOEF values to changes in temperature indicates qualitatively that a distribution is required. The agreement obtained at both fields verifies the assumption that a distribution of correlation times is required to reproduce the experimental data. For temperatures below 40 °C the distribution of correlation times is extremely broad; it remains relatively broad for this sample even at the highest temperatures studied. Below 10 °C, the backbone methylene resonance line width becomes quite large, making a T_1 determination very difficult, and thus evaluation of p was not practical. The increase in p value (which corresponds to a narrowing of the distribution) with increasing temperature is consistent with previous polymer studies.[28,29]

Hatada et al.[43] have recently reported data on a series of poly(alkyl methacrylates) in toluene-d_8 at 110 °C. They found

Table VI. ^{13}C Spin–Lattice Relaxation Times of Poly(*n*-hexyl methacrylate) in 20% (w/w) Solution in Toluene-d_8

Temp, °C	T_1 (67.9 MHz), s								
	C-1	C-2	C-3	C-4	C-5	C-6	CCH_3	CCH_2	CCR_4
16	0.26	0.27	0.54	0.87	1.4	2.1	0.049	0.084	1.6
22	0.25	0.28	0.55	1.0	1.5	2.4	0.057	0.079	1.3
35	0.24	0.35	0.67	1.2	2.0	2.8	0.060	0.063	1.2
65	0.30	0.60	1.4	2.4	3.6	4.3	0.099	0.067	1.2
91	0.37	0.92	2.0	4.2	5.0	6.8	0.18	0.081	1.5

Table VII. Observed and Calculated NT_1 and NOEF values for PBMA (50% in Toluene-d_8) as a Function of Temperature Assuming a Log $-\chi^2$ Distribution

Temp, °C	67.9 MHz				22.7 MHz					
	NT_1		NOEF		NT_1		NOEF			
	Calcd	Obsd	Calcd	Obsd	Calcd	Obsd	Calcd	Obsd	$\bar{\tau} \times 10^9$, s	Calcd width parameter
100	0.19	0.19	0.37	0.36	0.059	0.079	0.59	0.59	7.1	20
80	0.17	0.17	0.43	0.43	0.051	0.069	0.67	0.66	5.0	20
50	0.22	0.22	0.41	0.44	0.059	0.063	0.59	0.40	11	12
40	0.25	0.25	0.45	0.43	0.068	0.062	0.61		16	8
35[a]		0.27		0.56		0.062		0.30	~22[b]	
20[a]		0.34		0.63		0.067		0.31	~130[b]	

[a] p values for these temperatures are too low to be calculated with $b = 1000$. [b] Estimated values.

Table VIII. Calculated Methylene Spin-Lattice Relaxation Times and Nuclear Overhauser Enhancement Factors for the C-1 Carbon

Distribution width[a]	67.9 MHz		22.6 MHz		Exptl temp, °C[b]
	T_1, s	NOEF, η	T_1, s	NOEF, η	
$P = 8$ ($\tau = 1.3 \times 10^{-7}$ s)					
$D_1 = 1.2$	0.24	1.1	0.12	1.1	
$D_1 = 3.0$	0.34	1.1	0.16	1.1	
$P = 20$ ($\bar{\tau} = 5.0 \times 10^{-9}$ s)					See text
$D_1 = 1.2$	0.26	1.3	0.14	1.3	
$D_1 = 3.0$	0.40	1.3	0.21	1.2	
$P = 50$ ($\tau = 5.0 \times 10^{-9}$ s)					
$D_1 = 1.2$	0.29	1.3	0.15	1.2	
$D_1 = 3.0$	0.46	1.2	0.21	1.0	

[a] Log $-\chi^2$ distribution assumed; all D_i's are given in units of 10^{10} s^{-1}. [b] For PBMA and PHMA. Listed diffusion coefficients reproduce observed data for the stated experimental temperatures.

that the T_1s of the carbons were always longer in the isotactic polymer than in the syndiotactic one. The dependence of T_1s on tacticity has been noted previously for PMMA and polypropylene[44] while for polystyrene,[45,46] poly(vinyl alcohol),[47] and polyacrylonitrile[47] no dependence on steric configuration has been found within experimental error.

While our data for PBMA are comparable to Hatada's for poly(*tert*-butyl methacrylate) at 110 °C there is an apparent discrepancy in the NOEFs. They obtained maximum enhancement factors (~2) for all carbons of PMMA and consequently analyzed their data in terms of the single correlation time approximation assuming that the extreme narrowing condition was satisfied. Heatley and Begum[29] reported an NOEF of approximatly 1.2 (obtained from an interpolation of their plot; see Figure 5 of ref 29) for the backbone methylene carbon at comparable temperatures. This fact, in conjunction with the T_1 data, was used to satisfactorily analyze their data in terms of a distribution of correlation times. Our results confirm this latter behavior for the methacrylates (butyl and hexyl) while adding further strong evidence for the distribution approach, namely, the frequency dependence. Lyerla et al.[44b] have recently investigated PMMA at 38 and 100 °C and confirmed the applicability of the distribution model for this polymer.

We will not dwell at this point on the exact nature of the backbone motions which result in the observed phenomenological distribution theory being an appropriate model. The remaining discussion will address the question of whether side-chain substituents are affected by the distribution, and, if so, to what extent.

CCH_3. The trends exhibited by the methyl group directly attached to the backbone can be reproduced by a model which incorporates dependent internal rotation of the substituent attached to a backbone whose overall molecular motion must be described in terms of a distribution of correlation times.[29] In fact, comparison of the data obtained by Heatley and Begum[29] for poly(methyl methacrylate) (PMMA, 400 mg/mL in *o*-dichlorobenzene at 25.14 MHz) with our data for PBMA (Table I) reveals a striking similarity. The methyl substituent and main-chain methylene carbon T_1 data are virtually identical (allowing for the frequency differences) over a comparable temperature range. Furthermore, this correlation extends to PHMA (Table III) at the lower frequency.

Previous studies on related methyl groups have pointedly illustrated the varied behavior of methyl substituents. The correlation time of the methyl group in poly(propylene oxide)[29] was found to be independent of the average correlation time of the backbone while the methyl in poly(isobutylene)[29] exhibits an internal correlation time which is proportional to the backbone correlation time. The latter is similar to the situation for PMMA, PBMA, and PHMA.

C-1 Carbons. No attempt was made to fit all data *exactly* by making small incremental adjustments in the p parameter, the internal motion diffusion constants, or the average correlation times. The purpose of the present analysis is the determination of the relative importance of the complex motion for the backbone carbons as compared with the effects of multiple internal rotations about the C–C bonds. It should suffice to choose values for the parameters which encompass the extremes of measured T_1 and NOE values and hence the extremes of temperature. Numerous parameters have been varied to illustrate their effects and to elucidate whether all trends in the large experimental data set are satisfactorily reproduced.

T_1 data for the C-1 carbons in both polymers indicate an insensitivity to changes in temperature at both fields. In addition there is a great similarity in the magnitude and frequency dependence of the T_1 values when comparing PBMA and PHMA. Considering the change of correlation times and distribution widths associated with a temperature change of 100 °C, it should be considered remarkable if our calculations reasonably predict the relaxation behavior for all measured carbons.

Table VIII summarizes the numerical results for the C-1 carbon with a set of parameters ($\bar{\tau}$, p) chosen from the experimental results for two widely different temperatures. Therefore, the average correlation times span two orders of magnitude with the shorter correlation times (5×10^{-9} s) being associated with the narrower distribution parameters ($p = 50$ and $p = 20$) while the long correlation time is associated with the broad distribution width ($p = 8$) with $b = 1000$ in all cases.

For a large range in distribution widths and correlation times the calculated T_1s at a given field are relatively constant, even allowing for a moderate increase in the internal rotational diffusion constant (D_1) with increasing temperature.

The observed T_1s differ in value by a factor of 2–3 at the two magnetic field strengths, a trend which can be reproduced with the parameters of Table VIII.

The nuclear Overhauser enhancement factors are calculated to be in the range 1.0–1.3 for the given parameters, but inspection of the data reveals that a much wider range of values is observed as evidenced by the extreme values obtained at the highest and lowest temperatures for both polymers. While the calculated NOEFs are within experimental error of those observed ($\pm 0.3\eta$) for most of the intermediate temperatures, the deviations from calculated values at the highest and lowest temperatures are definitely outside of experimental error. This constituted the least satisfactory individual case (C-1 NOEFs at extreme temperatures) for the theory described in this paper.

Figure 11 illustrates the fact that for short correlation times (high temperatures) the NOEF at 22.6 MHz is greater than the NOEF at 67.9 MHz. This is the situation one predicts (and observes) for a system which can be described by a single correlation time or a simple distribution of correlation times. The more complex behavior observed in the present case can be attributed to the effect of internal rotation superimposed upon the overall molecular motion. Note that as the correlation times increase from ca. 5×10^{-10} s (as the temperature decreases) the NOEF difference for the two magnetic field strengths becomes smaller. Finally, at correlation times longer than $\sim 2.0 \times 10^{-9}$ s (for the given D_i) the NOEF at 67.9 MHz becomes greater by a substantial amount, the differences diminishing somewhat for very long correlation times.

The experimental data verify this behavior qualitatively (Table II). The NOEF for C-1 of PBMA at 67.9 MHz and −5 °C is at its maximum value (2.0η) while the 22.6-MHz NOEF is 0.47. As the temperature is increased the trends reverse, above 60 °C the NOEFs at 22.6 MHz being increasingly greater than those obtained at 67.9 MHz.

Theoretically, the presence of the motional distribution levels the NOEFs but the effects of the internal rotation can effectively negate this. The net result is that our theoretical modification emphasizes the effect of the distribution in a manner contrary to observation at the lowest temperatures.

Anisotropy in the backbone motions[19,38] can introduce an additional angular factor in the calculations. It has been shown that changing the angle between the first bond and the molecular z axis (assuming the symmetric rotor model) can affect the relaxation times considerably as a function of the anisotropy. This possibility has not been included in the present calculations and may partially obviate the discrepancies, particularly for C-1 since the effects of anisotropic motion are calculated to be greatest at this chain position.

For a constant diffusion coefficient the WLL theory predicts that the side-chain T_1s will increase as the temperature decreases (within the calculated range of correlation times for PBMA and PHMA). While this is not in fact the case, it should be noted that an insensitivity to temperature may result from the WLL theory provided that the diffusion constants decrease enough to offset the increase due to the longer backbone correlation times.

C-2 Carbons. For similar temperatures the C-2 carbon T_1s of PBMA are larger than the corresponding values for PHMA. This is consistent with the greater internal motional freedom associated with a shorter chain, lessening the effects of inter- and intramolecular interactions due to chain entanglements. However, the glass transition temperature of PHMA is lower than that of PBMA[48] so that direct and absolute comparison of the polymers at similar temperatures is not free of ambiguity as to the origin of differences in dynamics.

The frequency dependence of the T_1s for C-2 is not as great on the average as that observed for C-1 but is still of considerable magnitude and outside experimental error. Inspection of Table IX in conjunction with Tables I and III reveals that the distribution modified internal rotation theory is able to predict the frequency-dependent behavior for C-2.

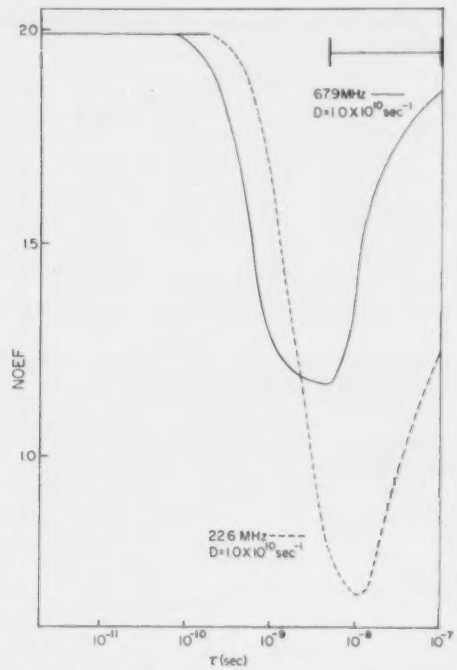

Figure 11. Nuclear Overhauser enhancement factors for C-1 carbon undergoing internal rotation as a function of the isotropic correlation time for backbone motion at 22.635 (- - - - -) and 67.905 MHz (—). $D_i = 1 \times 10^{10}$ s^{-1}. Single correlation time model used.

The NOEFs (Tables II, IV) do not exhibit the trends that were so obvious for C-1. They tend to average $\sim 1.5 \pm 0.3\eta$ (except for the temperature extremes at 67.9 MHz). Table IX shows that the effective distribution width is still broad ($p = 20$) for C-2. (A larger value of p, approaching the WLL theory, would result in predicted NOEFs which are consistently larger than the observed values while predicting a small or negligible frequency dependence, also contrary to observations.)

Under certain circumstances (see Tables I, III, and V) the C-2 carbon T_1s in PBMA and PHMA are shorter than the T_1s for C-1 and C-3 at the same temperature. The effect is greatest at low temperatures and the higher magnetic field strength. (At 67.9 MHz the effect disappears for temperatures above 20–40 °C, depending on the sample.)

Doddrell et al.[8] have shown that increasing the rate of internal rotation can result in a decrease in T_1 if the backbone (chain) motion satisfies the condition $\omega^2\tau^2 \gg 1$ in conjunction with the condition $\omega^2\tau^2_{\text{eff}} \sim 1$ for the side-chain carbon undergoing the internal rotation. The latter condition is not a necessary condition for observation of the phenomenon. Even for $\omega^2\tau^2_{\text{eff}} \ll 1$ the effect may occur. Levine et al.[18,19] have proposed the following explanation. "The transformation along the chain effectively attenuates the correlation function of the molecular motion, leading to an increase in the spectral density at high frequencies and for carbon 2 this increase is greater than the accompanying decrease in spectral density due to the internal motions leading to a net increase in spectral density at high frequencies, and thus, to a reduction in T_1."

It was noted[19] that the effect is very sensitive to the Larmor frequencies involved. Thus (at 23 kG) the effect was seen for ^{1}H-^{1}H relaxation but not for ^{13}C-^{1}H relaxation. This is consistent with the fact that the C-2 T_1s of PBMA and PHMA decrease relative to C-1 only at the higher field (higher Larmor frequency) and only at certain temperatures (for which the condition $\omega^2\tau^2 \gg 1$ is satisfied).

C-3 Carbons. Not until C-3 is reached do the greatest dif-

Table IX. Calculated Methylene Spin–Lattice Relaxation Times and Nuclear Overhauser Enhancement Factors for the C-2 Carbon

Distribution width[a]	67.9 MHz		22.6 MHz		Exptl temp, °C[b]	
	T_1, s	NOEF, η	T_1, s	NOEF, η	PBMA	PHMA
$P = 8$						
($\bar{\tau} = 1.3 \times 10^{-7}$ s)						
$D_1 = 1.2, D_2 = 3.0$	0.36	1.2	0.20	1.3		34
$D_1 = 1.2, D_2 = 5.0$	0.41	1.2	0.22	1.3	21	43
$D_1 = 1.2, D_2 = 10.0$	0.48	1.3	0.26	1.3		
$P = 20$ ($\bar{\tau} = 5.0 \times 10^{-9}$ s)						
$D_1 = 1.2, D_2 = 3.0$	0.52	1.6	0.37	1.6	46	63
$D_1 = 1.2, D_2 = 5.0$	0.62	1.6	0.44	1.6	55	83
$D_1 = 1.2, D_2 = 10.0$	0.75	1.6	0.53	1.6		100
$P = 50$ ($\bar{\tau} = 5.0 \times 10^{-9}$ s)						
$D_1 = 1.2, D_2 = 1.0$	0.51	1.8	0.40	1.7		
$D_1 = 1.2, D_2 = 3.0$	0.78	1.8	0.60	1.6		
$D_1 = 1.2, D_2 = 5.0$	0.92	1.7	0.69	1.6	98	
$D_1 = 1.2, D_2 = 10.0$	1.13	1.7	0.81	1.5		

[a] Log $-\chi^2$ distribution assumed; all D_i's are given in units of 10^{10} s^{-1}. [b] Listed diffusion coefficients reproduce observed data for the stated experimental temperatures.

Table X. Calculated Methylene Spin–Lattice Relaxation Times and Nuclear Overhauser Enhancement Factors for the C-3 Carbon

Distribution width[a]	67.9 MHz		22.6 MHz		Exptl temp, °C[b]	
	T_1, s	NOEF, η	T_1, s	NOEF, η	PBMA	PHMA
$P = 8$						
($\bar{\tau} = 1.3 \times 10^{-7}$ s)						
$D_1 = 1.2, D_2 = 5.0, D_3 = 5.0$	0.59	1.3	0.34	1.4		34
$D_1 = 1.2, D_2 = 5.0, D_3 = 7.0$	0.63	1.3	0.37	1.4		
$D_1 = 1.2, D_2 = 5.0, D_3 = 10.0$	0.69	1.3	0.40	1.4	21	43
$P = 20$ ($\bar{\tau} = 5.0 \times 10^{-9}$ s)						
$D_1 = 1.2, D_2 = 5.0, D_3 = 5.0$	1.18	1.7	0.96	1.8	46	63
$D_1 = 1.2, D_2 = 5.0, D_3 = 7.0$	1.30	1.7	1.08	1.8		83
$D_1 = 1.2, D_2 = 5.0, D_3 = 10.0$	1.47	1.7	1.21	1.8	55	
$P = 50$ ($\bar{\tau} = 5.0 \times 10^{-9}$ s)						
$D_1 = 1.2, D_2 = 5.0, D_3 = 5.0$	2.20	1.9	2.00	1.9		
$D_1 = 1.2, D_2 = 5.0, D_3 = 7.0$	2.47	1.9	2.24	1.8		
$D_1 = 1.2, D_2 = 5.0, D_3 = 10.0$	2.80	1.9	2.51	1.8	98	

[a] Log $-\chi^2$ distribution assumed; all D_i's are given in units of 10^{10} s^{-1}. [b] Listed diffusion coefficients reproduce observed data for the stated experimental temperatures.

Table XI. Calculated Methylene Spin–Lattice Relaxation Times and Nuclear Overhauser Enhancement Factors for the C-3 Carbon

Distribution width[a]	67.9 MHz		22.6 MHz		Exptl temp, °C[b]
	T_1, s	NOEF, η	T_1, s	NOEF, η	PBMA
$P = 8$					
($\bar{\tau} = 1.3 \times 10^{-7}$ s)					
$D_1 = 1.2, D_2 = D_3 = 10.0$	0.78	1.4	0.46	1.4	21
$D_1 = 1.2, D_2 = 10.0, D_3 = 30.0$	1.03	1.4	0.62	1.4	37
$D_1 = 1.2, D_2 = 10.0, D_3 = 70.0$	1.30	1.4	0.79	1.4	46
$P = 20$ ($\bar{\tau} = 5.0 \times 10^{-9}$ s)					
$D_1 = 1.2, D_2 = D_3 = 10.0$	1.80	1.8	1.49	1.8	
$D_1 = 1.2, D_2 = 10.0, D_3 = 30.0$	2.61	1.7	2.13	1.8	
$D_1 = 1.2, D_2 = 10.0, D_3 = 70.0$	3.39	1.7	2.70	1.7	
$P = 50$ ($\bar{\tau} = 5.0 \times 10^{-9}$ s)					
$D_1 = 1.2, D_2 = D_3 = 10.0$	3.49	1.9	3.06	1.8	
$D_1 = 1.2, D_2 = 10.0, D_3 = 30.0$	5.00	1.8	4.18	1.7	
$D_1 = 1.2, D_2 = 10.0, D_3 = 70.0$	6.24	1.8	5.00	1.7	

[a] Log $-\chi^2$ distribution assumed; all D_i's are given in units of 10^{10} s^{-1}. [b] Listed diffusion coefficients reproduce observed data for the stated experimental temperatures.

ferences among the available theories become apparent. The WLL theory predicts that a virtually maximum NOEF should be observed for C-3 with the correlation times spanned by the backbone carbons. However, a consistently reproducible NOEF which is *less than the maximum value* is observed for PHMA (Table IV). While data are not available for C-3 of PBMA, interpolation from the C-2 and C-4 NOEFs confirms a similar trend for PBMA. It is not reasonable to expect that the C-3 NOEFs of PBMA could vary greatly from the average values of the C-2 and C-4 NOEFs since the values for these latter carbons are generally so close over the entire temperature range studied.

The frequency dependence of the C-3 T_1s is again considerable for both polymers. For p values $\gtrsim 50$, one predicts (Tables X and XI) that the frequency dependence is quite small, vanishing for the single correlation time (WLL) theory.

Table XII. Calculated Methylene Spin–Lattice Relaxation Times and Nuclear Overhauser Enhancement Factors for the C-4 Carbon

Distribution width[a]	67.9 MHz		22.6 MHz		Exptl temp, °C[b]
	T_1, s	NOEF, η	T_1, s	NOEF, η	PHMA
$P = 8$					
($\bar{\tau} = 1.3 \times 10^{-7}$ s)					
$D_1 = 1.2, D_2 = D_3 = D_4 = 5.0$	0.74	1.4	0.44	1.4	
$D_1 = 1.2, D_2 = 5.0, D_3 = 7.0,$ $D_4 = 10.0$	0.87	1.4	0.53	1.4	
$D_1 = 1.2, D_2 = 5.0, D_3 = 10.0,$ $D_4 = 30.0$	1.18	1.4	0.73	1.4	34
$P = 20$					
($\bar{\tau} = 5.0 \times 10^{-9}$ s)					
$D_1 = 1.2, D_2 = D_3 = D_4 = 5.0$	1.74	1.8	1.51	1.9	49
$D_1 = 1.2, D_2 = 5.0, D_3 = 7.0,$ $D_4 = 30.0$	2.28	1.8	2.01	1.9	
$D_1 = 1.2, D_2 = 5.0, D_3 = 10.0,$ $D_4 = 30.0$	3.58	1.8	3.19	1.9	
$P = 50$					
($\bar{\tau} = 5.0 \times 10^{-9}$ s)					
$D_1 = 1.2, D_2 = D_3 = D_4 = 5.0$	3.64	2.0	3.56	2.0	
$D_1 = 1.2, D_2 = 5.0, D_3 = 7.0,$ $D_4 = 10.0$	4.95	2.0	4.82	2.0	
$D_1 = 1.2, D_2 = 5.0, D_3 = 10.0,$ $D_4 = 30.0$	7.98	2.0	7.68	2.0	

[a] Log $-\chi^2$ distribution assumed; all D_i's are given in units of 10^{10} s^{-1}. [b] Listed diffusion coefficients reproduce observed data for the stated experimental temperatures.

Table XIII. Calculated Methyl Spin–Lattice Relaxation Times and Nuclear Overhauser Enhancement Factors for the C-4 Carbon

Distribution width[a]	67.9 MHz		22.6 MHz		Exptl temp, °C[b]
	T_1, s	NOEF, η	T_1, s	NOEF, η	PBMA
$p = 8$					
($\bar{\tau} = 1.3 \times 10^{-7}$ s)					
$D_1 = 1.2, D_2 = 5.0, D_3 = 10.0,$ $D_4 = 30.0$	0.79	1.4	0.49	1.4	
$D_1 = 1.2, D_2 = 10.0, D_3 = 10.0,$ $D_4 = 30.0$	0.84	1.4	0.53	1.5	
$p = 20$					
($\bar{\tau} = 5.0 \times 10^{-9}$ s)					
$D_1 = 1.2, D_2 = 5.0, D_3 = 10.0,$ $D_4 = 30.0$	2.39	1.8	2.13	1.9	66
$D_1 = 1.2, D_2 = 10.0, D_3 = 10.0,$ $D_4 = 30.0$	2.69	1.8	2.42	1.9	83
$p = 50$					
($\bar{\tau} = 5 \times 10^{-9}$ s)					
$D_1 = 1.2, D_2 = 5.0, D_3 = 10.0,$ $D_4 = 30.0$	5.32	2.0	5.12	1.9	
$D_1 = 1.2, D_2 = 10.0, D_3 = 10.0,$ $D_4 = 30.0$	6.11	2.0	5.86	1.9	

[a] Log $-\chi^2$ distribution assumed; all D_i's are given in units of 10^{10} s^{-1}. [b] Listed diffusion coefficients reproduce observed data for the stated experimental temperatures.

The low- and intermediate-temperature data are reproduced quite well by inclusion of the distribution effects ($p \simeq 8$–20, as determined above), particularly for PHMA. However, the frequency dependence of the T_1s for PBMA at high temperatures ($\gtrsim$90 °C) cannot be reproduced with a reasonable set of parameters; the previously determined backbone distribution is too narrow to quantitatively accommodate the observed differences.

C-4 Carbons. The C-4 carbon of PBMA is a methyl group and, therefore, direct comparison with the C-4 carbon of PHMA is not possible in the manner chosen for carbons C-1 through C-3. Table XII gives representative calculations for the C-4 carbon of PHMA. Table XIII specifically illustrates the calculated methyl T_1 values for a C-4 carbon with the given parameters; hence the observed T_1s of Table I for PBMA can be compared directly.

The low-temperature ($\lesssim$50 °C) frequency dependence of the T_1s is reasonably predicted by our theory, i.e., the T_1s vary by approximately 20% with the change in frequency from 22.6 to 67.9 MHz. At high temperatures the frequency dependence for C-4 *increases* in relative magnitude; this cannot be successfully predicted by this or any other theory presently known. The trends in T_1 are illustrated in Figure 12.

The implication follows that the terminal methyl has associated with it some very long correlation times. A gradual loss of a frequency dependence under our present theoretical assumptions does not correspond with the observed situation. Obviously, factors that are as yet unaccounted for contribute significantly to the dynamic behavior of the terminal methyl group.

One is reminded at this point of the results of Levine[36] which predicted that a strong correlation in the motions of pairs of

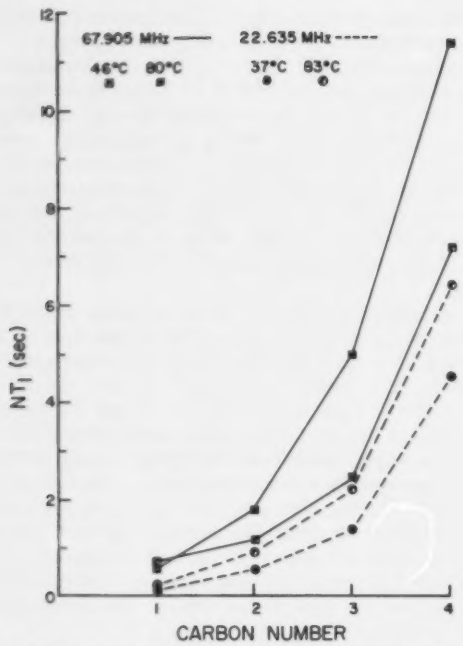

Figure 12. NT_1 values for side-chain carbons of poly(*n*-butyl methacrylate) 50% w/w in toluene-d_8 at 67.9 MHz (46, 80 °C) and 22.6 MHz (37, 83 °C).

C–H vectors on adjacent atoms may be possible. Thus, the C-4 carbon of PBMA could be considered as interacting with the C-3 carbon and acquiring characteristics indicative of the C-3 carbon, including an increased frequency dependence for comparable diffusion coefficients.

The origin of the unusual T_1s observed in these polymers for C-4 is not reflected in any precipitous changes in nuclear Overhauser enhancement factors at this position. The experimental values are still less than maximum, as predicted by distribution widths $\lesssim p = 20$.

C-5 and C-6 Carbons (PHMA Only). The NOEFs for C-5 (Table XIV) can be predicted from the relatively broad distribution width associated with the backbone carbon T_1s. As noted in the numerical results section the relative insensitivity of the NOEFs for broad distributions is predicted to extend quite a distance from carbon 0 for reasonable diffusion coefficients. The same can be said for the C-6 carbon. Despite NT_1 values of the order of 20.0 s the NOEFs appear to be less than maximum (Table IV).

The low-temperature C-5 T_1 and NOE results are in accord with our theoretical predictions, particularly for temperatures $\lesssim$50 °C. However, for higher temperatures the T_1 frequency dependence cannot be quantitatively predicted; the experimental differences are larger than theory predicts.

The situation is similar with respect to the C-6 carbon T_1 data. For a sufficiently long chain (using a relatively narrow distribution width) theory predicts a gradual loss of the frequency dependence of the spin–lattice relaxation time. While the end methyl of PHMA does exhibit frequency-dependent T_1s they too are underestimated slightly by the present theoretical approach. We are therefore investigating improvements that will try to alleviate this deficiency.

The overall trends support the likelihood that further improvement in the theory can be made by treating the trans-gauche conformational changes explicitly[19b,36,37,50] despite the fact that the assumption of independent bond rotation in conjunction with stochastic rotational diffusion has been relatively successful[18,19,38] for interpreting the chain dynamics of various compounds.

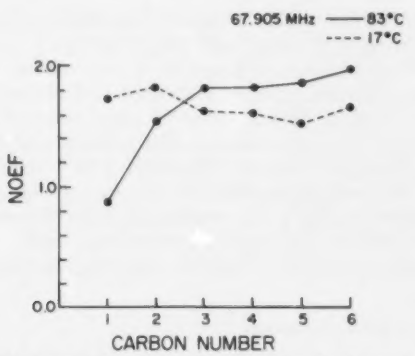

Figure 13. Nuclear Overhauser enhancement factors for side-chain carbons of poly(*n*-hexyl methacrylate) 50% w/w in toluene-d_8 at 67.9 MHz (83, 17 °C).

Table XIV. Calculated Methylene Spin–Lattice Relaxation Times and Nuclear Overhauser Enhancement Factors for the C-5 Carbon

Distribution width[a]	67.9 MHz T_1, s	67.9 MHz NOEF, η	22.6 MHz T_1, s	22.6 MHz NOEF, η
$P = 8$ ($\bar{\tau} = 1.3 \times 10^{-7}$ s)				
$D_1 = D_2 = D_3 = D_4 = D_5 = 1.0$	0.43	1.3	0.25	1.4
$D_1 = D_2 = D_3 = 1.0$, $D_4 = 4.0$, $D_5 = 7.0$	0.68	1.3	0.46	1.4
$D_1 = D_2 = D_3 = D_4 = D_5 = 10.0$	1.43	1.4	0.91	1.5
$P = 20$ ($\bar{\tau} = 5.0 \times 10^{-9}$ s)				
$D_1 = D_2 = D_3 = D_4 = D_5 = 1.0$	0.74	1.7	0.60	1.8
$D_1 = D_2 = D_3 = 1.0$, $D_4 = 4.0$, $D_5 = 7.0$	1.50	1.8	1.29	1.9
$D_1 = D_2 = D_3 = D_4 = D_5 = 10.0$	5.25	1.9	4.88	1.9

[a] Log $-\chi^2$ distribution assumed; all D_i's are given in units of 10^{10} s^{-1}.

For instance, lipid bilayer motion has been treated[50] as fast β-coupled gauche isomerization of sets of carbon bonds superimposed on slow, nearly isotropic chain reorientations with some success. However, in this latter case[50] full NOEFs were observed and a more elaborate theory involving more cooperative molecular motions is not justified. It remains to be determined whether the spin–lattice relaxation times are frequency dependent in systems of this type since an essentially complete NOEF (1.8–1.9, for example), in conjunction with a relatively large NT_1, does not guarantee that the extreme narrowing condition can be invoked with certainty.

Cross Correlation Effects. Cross correlation effects (even under proton decoupled conditions) should be most evident for methylene carbons undergoing anisotropic reorientation with correlation times that are of the order of $\omega_C \sim 6D_o$ where D_o is the diffusion constant for overall motion of the molecule and ω_C is the Larmor frequency of carbon. London et al.[20] have shown that, except for C-1, the effects are insignificant for internal diffusion constants, D_i, equal to 10^9 s^{-1} but they become more important for $D_i = 10^{10}$ and 10^{11} s^{-1}. This is particularly true for carbons C-1 through C-3. There also can be significant nonexponential spin–lattice relaxation.[20] The conditions for which maximum deviations from "normal" behavior occur are characterized by overall molecular diffusion of ca. 10^7–10^8 s^{-1} and internal rotational diffusion constants of $\sim 10^{10}$ s^{-1}.

Cross correlation effects are attenuated as the carbon under

consideration becomes more remote from the site of substitution to the main chain carbons. Examination of the data in Table VII shows that the range $D_0 = \sim 10^6$–10^8 s^{-1} for the backbone diffusion constant is covered in the experimental temperature range. This is precisely the most sensitive region[20] for detection of cross correlation effects. In addition the rotational diffusion constants are of the order of 10^{10}–10^{11} s^{-1} (vide supra). The predicted deviation due to cross correlation effects (neglecting the effects of a distribution of correlation times) in the NOEF for C-1 (and C-2) under these conditions is approximately 0.2–0.5 units. The data show no evidence for these effects.

Summary and Conclusions

1. Invocation of a distribution of correlation times for the backbone carbons of PHMA and PBMA yields a satisfactory fit of the main-chain experimental relaxation data at two fields and over a large range of temperatures. This is the situation anticipated for molecules of the type studied.

2. The single correlation time, extreme narrowing, approximation can be inadequate for description not only of the dynamic behavior of polymer backbone carbons, but also for alkyl (or related) side-chain substituents.

3. Carbons which are, strictly speaking, eight bonds removed from the polymer backbone exhibit frequency-dependent relaxation times and less than maximum nuclear Overhauser enhancement factors.[44] This is the most unique aspect of the data presented and of prime consideration in any theory which is developed for structures related to these compounds.

4. Multiple internal rotation effects alone *cannot* account for the observed side-chain NMR parameters.

5. A distribution of correlation times for the backbone carbons is effective in altering the dynamic parameters of well-removed side-chain carbons, inducing frequency-dependent T_1 and NOE behavior.

6. The inability to quantitatively fit the high-temperature spin–lattice relaxation times for the end methyls (PHMA, PBMA) and penultimate carbon of PHMA indicates that the present theoretical modifications, while more predictive than previous theories, do not always quantitatively assess the effects of complex motions. The assumptions of independent bond rotations and/or stochastic diffusion (although presently required for practical calculations) may be inadequate.

7. Alkyl chain dynamics (in various environments) as measured by NMR require quite different motional models. One model should not be expected to uniquely determine the NMR parameters in different polymers. In fact it is conceivable that the sample state (solvent,[51] concentration, temperature, etc.) could be a more crucial factor in governing which model is most applicable to a particular system. For instance, the causative factors which result in an unusually large frequency dependence for the chain ends in PBMA and PHMA may be intramolecular or intermolecular. Extensive dilution studies will be required to solve this problem.

8. Unlike the *n*-alkanes[18,19,42b] the relaxation data cannot be interpreted by a model in which the diffusion constants for internal rotation are the same for all bonds. The data are better explained in terms of a *slower* diffusion constant for the first bond and slightly increasing diffusion constants for the remaining methylene carbons. The terminal methyl data require a large increase in internal rotation about the CH_2–CH_3 bond (see also ref 42b).

Studies of hydrocarbon chains in dipalmitoyllecithin bilayers[3] provide an interesting comparison in that the motions of the chain near the terminal methyl are identical with the motion for corresponding *n*-alkane carbons (and in qualitative agreement with the present calculated diffusion constants). Most significant is the observation that the motions of the C–C bonds near the glycerol bridge of the lipids are an order of magnitude slower than the remaining chain carbons.

It has been suggested[3] that the slow motions required to fit the observed data in this and other cases may be oscillatory in nature ("librations") rather than involving effective full-bond rotations. Under these circumstances the correlation time is the product of the true motional correlation time and a factor describing the amplitude and rate of the oscillatory motion. Unfortunately, it is not currently possible to distinguish an increase in the true rotational diffusion constant from an increase in the amplitude and rate of oscillatory motion along the chain.

The problem concerning an absolute choice of model for rotation about the carbon–carbon single bonds of an alkyl chain may be intractable. Many models have been proposed to explain, in a more fundamental manner, the detailed mechanism by which internal motion occurs for polymeric chains in both the crystalline and noncrystalline states. The ability of a single technique to distinguish among the multitudinous possibilities has not been demonstrated as yet. The available NMR data generally lend themselves to numerous reasonable interpretations. One is also faced with providing a tractable, hopefully general, theoretical interpretation which is applicable by others to their own particular problems without undue expense in terms of time (theoretical complexity) or money (computer simulation).

Finally, it is hoped that presentation of the available data over a wide range of temperatures at two different magnetic fields will allow others to test various models more completely.

Acknowledgments. We would like to acknowledge helpful discussions with Dr. J. Lewis and Professors Jim Prestegard and Leo Mandelkern. Financial support from the National Science Foundation and U.S. Environmental Protection Agency is gratefully acknowledged.

References and Notes

(1) Alfred P. Sloan Fellow, 1975–1977; Camille and Henry Dreyfus Teacher-Scholar, 1976–1981.
(2) R. L. Somorjai and R. Deslauriers, *J. Am. Chem. Soc.*, **98**, 6460 (1976).
(3) Y. K. Levine, P. Partington, G. C. K. Roberts, N. J. M. Birdsall, A. G. Lee, and J. C. Metcalfe, *FEBS Lett.*, **23**, 203 (1972).
(4) Y. K. Levine, N. J. M. Birdsall, A. G. Lee, and J. C. Metcalfe, *Biochemistry*, **11**, 1416 (1972); J. D. Robinson, N. J. M. Birdsall, A. G. Lee, and J. C. Metcalfe, *ibid.*, **11**, 2903 (1972).
(5) G. C. Levy, T. Holak, and A. Steigel, *J. Am. Chem. Soc.*, **98**, 495 (1976), and earlier papers.
(6) A. Abragam, "The Principles of Nuclear Magnetism", Oxford University Press, London, 1961, Chapter 8.
(7) T. C. Farrar and E. D. Becker, "Pulse and Fourier Transform NMR", Academic Press, New York, N.Y., 1971.
(8) D. Doddrell, V. Glushko, and A. Allerhand, *J. Chem. Phys.*, **56**, 3683 (1972).
(9) J. Grandjean and P. Laszlo, *Mol. Phys.*, **30**, 413 (1975).
(10) A. Allerhand and R. A. Komoroski, *J. Am. Chem. Soc.*, **95**, 8228 (1973).
(11) H. Saito, H. H. Mantsch, and I. C. P. Smith, *J. Am. Chem. Soc.*, **95**, 8453 (1973).
(12) M. C. Fedarko, *J. Magn. Reson.*, **12**, 30 (1973).
(13) G. C. Levy, *Acc. Chem. Res.*, **6**, 161 (1973).
(14) S. Berger, F. R. Kreissl, D. M. Grant, and J. D. Roberts, *J. Am. Chem. Soc.*, **97**, 1805 (1975).
(15) D. E. Woessner and B. S. Snowden, Jr., *Adv. Mol. Relaxation Processes*, **3**, 181 (1972).
(16) D. E. Woessner, *J. Chem. Phys.*, **36**, 1 (1962).
(17) D. Wallach, *J. Chem. Phys.*, **47**, 5258 (1967).
(18) Y. K. Levine, P. Partington, and G. C. K. Roberts, *Mol. Phys.*, **25**, 497 (1973).
(19) (a) Y. K. Levine, N. J. M. Birdsall, A. G. Lee, J. C. Metcalfe, P. Partington, and G. C. K. Roberts, *J. Chem. Phys.*, **60**, 2890 (1974); (b) A. G. Lee, N. J. M. Birdsall, J. C. Metcalfe, G. B. Warren, and G. C. K. Roberts, *Proc. R. Soc. London, Ser. B*, **193**, 253 (1976).
(20) R. E. London and J. Avitabile, *J. Chem. Phys.*, **65**, 2443 (1976), note that there is an apparent typographical error in the given B_{00} element in that the whole term should be squared.
(21) W. T. Huntress, Jr., *J. Chem. Phys.*, **48**, 3524 (1968).
(22) L. G. Werbelow and D. M. Grant, *J. Chem. Phys.*, **63**, 544 (1975).
(23) L. G. Werbelow and D. M. Grant, *J. Chem. Phys.*, **63**, 4742 (1975).
(24) D. Canet, G. C. Levy, and I. R. Peat, *J. Magn. Reson.*, **18**, 199 (1975). (Actually, because of the large range of T_1s found in each of these polymer

solutions, the designated experiments met the requirements for conventional inversion-recovery ($T \gtrsim 4T_1$) for all carbons except the last one or two carbons of the side chain.)
(25) R. Freeman, H. D. W. Hill, and R. Kaptein, *J. Magn. Reson.*, **7**, 327 (1972); S. J. Opella, D. J. Nelson, and O. Jardetzky, *J. Chem. Phys.*, **64**, 2533 (1976); R. K. Harris and R. H. Newman, *J. Magn. Reson.*, **24**, 449 (1976).
(26) (a) T. M. Connor, *Trans. Faraday Soc.*, **60**, 1574 (1964); (b) J. Mikayke, *J. Polym. Sci.*, **28**, 477 (1958).
(27) K. S. Cole and R. H. Cole, *J. Chem. Phys.*, **9**, 341 (1944).
(28) J. Schaefer, *Macromolecules*, **6**, 882 (1973).
(29) (a) F. Heatley and A. Begum, *Polymer*, **17**, 399 (1976); (b) F. Heatley and M. K. Cox, *ibid.*, **18**, 225 (1977).
(30) R. M. Fuoss and H. G. Kirkwood, *J. Am. Chem. Soc.*, **63**, 385 (1941).
(31) D. W. Davidson and R. H. Cole, *J. Chem. Phys.*, **18**, 1417 (1950); **19**, 1484 (1951).
(32) F. Noack, "NMR Basic Principles and Progress", Vol. 3, Springer-Verlag, New York, N.Y., 1971.
(33) J. R. Macdonald, *J. Chem. Phys.*, **36**, 345 (1962).
(34) The present theory may also be inadequate to describe molecular dynamics in strongly aggregated low molecular weight compounds, such as 1,2-decanediol: G. C. Levy, M. P. Cordes, J. S. Lewis, and D. E. Axelson, *J. Am. Chem. Soc.*, **99**, 5492 (1977).
(35) P. L. Meyer, "Introductory Probability and Statistical Applications", Addison-Wesley, Reading, Mass., 1970.
(36) Y. K. Levine, *J. Magn. Reson.*, **11**, 421 (1973).
(37) T. Yasukawa, D. Ghesquiere, and C. Chachaty, *Chem. Phys. Lett.*, **45**, 279 (1977).
(38) R. Deslauriers and R. L. Somorjai, *J. Am. Chem. Soc.*, **98**, 1931 (1976).
(39) D. Doddrell and A. Allerhand, *J. Am. Chem. Soc.*, **93**, 1558 (1971).
(40) E. Breitmaier, K-H Spohn, and S. Berger, *Angew. Chem., Int. Ed. Engl.*, **14**, 144 (1975).
(41) N. J. M. Birdsall, A. G. Lee, Y. K. Levine, J. C. Metcalfe, P. Partington, and G. C. K. Roberts, *J. Chem. Soc., Chem. Commun.*, 757 (1973).
(42) (a) C. Chachaty, Z. Wolkowski, F. Piriou, and G. Lukacs, *J. Chem. Soc., Chem. Commun.*, 951 (1973); (b) J. Lyerla, Jr., H. M. McIntyre, and D. A. Torchia, *Macromolecules*, **7**, 11 (1974).
(43) K. Hatada, Y. Okamoto, K. Ohta, Y. Ymemura, and H. Yuki, *Makromol. Chem.*, **178**, 617 (1977).
(44) (a) J. C. Randall, *J. Polym. Sci., Polym. Phys. Ed.*, **14**, 1693 (1976); (b) J. R. Lyerla, T. T. Horikawa, and D. E. Johnson, *J. Am. Chem. Soc.*, **99**, 2463 (1977).
(45) A. Allerhand and R. K. Hailstone, *J. Chem. Phys.*, **56**, 3718 (1972).
(46) J. Schaefer and D. F. S. Natusch, *Macromolecules*, **5**, 416 (1972).
(47) Y. Inoue, A. Nishioka, and R. Chujo, *J. Polym. Sci., Polym. Phys. Ed.*, **11**, 2237 (1973).
(48) J. D. Ferry, "Viscoelastic Properties of Polymers", Wiley, New York, N.Y., 1961; S. S. Rogers and L. Mandelkern, *J. Chem. Phys.*, **61**, 985 (1957).
(49) Preliminary data on a related polymer [poly(*n*-octyl acrylate)] indicate that ten bonds may be required in these polymers before relatively temperature independent NOEs are observed.
(50) M. P. N. Gent and J. H. Prestegard, *J. Magn. Reson.*, **25**, 243 (1977).
(51) Y. Inoue, T. Konno, R. Chujo, and A. Nishioka, *Makromol. Chem.*, **178**, 2131 (1977).